

## Magnetism and local order. II. Self-consistent cluster calculations

M. R. Press, Feng Liu, S. N. Khanna, and P. Jena

*Physics Department, Virginia Commonwealth University, Richmond, Virginia 23284-2000*

(Received 27 January 1989)

The effect of the local environment on the magnetic moment and its convergence to bulk value has been studied self-consistently by using a molecular-cluster model within the framework of spin-density-functional theory. We show that the magnetic moment of the central atom in clusters of 43 Ni atoms and 27 Fe atoms can reproduce the bulk values very well. The moments of atoms surrounding the central site increase as one approaches the surface—a consequence of decreasing coordination number. The defects such as vacancies and carbon and phosphorous impurities have a strong effect on the magnetic moment of the nearest host atom: The vacancies enhance the moments while the impurities quench them. The former is caused by a reduction in the coordination number, whereas the latter is caused by *pd* hybrids formed out of interacting impurity *p* and host *d* states. The effect of multiple defect complexes on the host magnetic properties has also been investigated, and the results are compared with available experimental data.

### I. INTRODUCTION

In a previous paper,<sup>1</sup> hereafter referred to as I, we have discussed the effect of the near-neighbor environment on the magnetic moments of Fe, Co, and Ni. The coordination number (defined as the number of atoms in the nearest-neighbor shell) of the magnetic atoms was varied by considering linear chains, surfaces, and thin films of different crystallographic directions. Using a simple and computationally efficient *ab initio* tight-binding method (ATB) we showed that the magnetic moments of atoms are significantly influenced by their local environment and that our results were in agreement with available experimental and other sophisticated theoretical results.

In this paper we have studied this problem from the point of view of clusters modeled as fragments of their crystalline structures. These studies illustrate two different but complementary aspects of the problem: the convergence of magnetic moments to bulk values as clusters grow and the effect of coordination number. These results also shed light on recent experiments on magnetic moments of free clusters.<sup>2</sup>

There have been many experimental studies<sup>3</sup> of the magnetic properties of transition metals containing impurities. Using the cluster technique, we have investigated the role impurities like carbon and phosphorous play on the magnetic properties of Fe and Ni. We are also able to identify the mechanisms underlying the demagnetization of host atoms adjacent to the impurities.

A brief outline of our theoretical procedure is given in Sec. II. The results of the electronic and magnetic properties of perfect and imperfect clusters of Fe and Ni are presented and discussed in Sec. III. A summary of our conclusions is contained in Sec. IV.

### II. THEORETICAL APPROACH

We have used the self-consistent-field linear combination of atomic orbitals molecular-orbital (SCF-LCAO-

MO) method within the density-functional formalism to carry out electronic structure calculations of  $Ni_n$ ,  $Fe_n$ ,  $Ni_nP$ , and  $Fe_nC_m$  clusters ( $n \leq 43$  for Ni and  $\leq 30$  for Fe,  $m \leq 2$  for C) confined to their bulk geometries. The Rayleigh-Ritz secular equation  $(\underline{H} - E\underline{S})\underline{C} = 0$  was solved using the discrete variational method<sup>4</sup> (DVM). In short, the DVM involves use of numerical atomic orbitals in the construction of molecular orbitals. In this work, orbital configurations  $3d^9$ ,  $4s^{0.99}$ , and  $4p^{0.01}$  for Ni,  $3d^7$ ,  $4s^{0.99}$ , and  $4p^{0.01}$  for Fe,  $3s^2$ ,  $3p^{2.99}$ , and  $3d^{0.01}$  for P, and  $2s^2$  and  $2p^2$  for C were employed to generate the valence orbitals for these atoms. The effect of the rest of the bulk was simulated through an embedding scheme.<sup>5</sup> The secular equation was then solved self-consistently using matrix elements obtained via three-dimensional numerical integrations performed on a grid of random points by the diophantine method. About 500 sampling points around Ni and Fe sites and 600 around P and C were employed. These points were found to be sufficient for convergence of the electronic spectrum to within 0.01 eV. The details of the method are well documented in literature<sup>4,5</sup> and are not reproduced here. The geometries of the Ni and Fe clusters studied here are given in Figs. 1 and 2, respectively.

### III. RESULTS AND DISCUSSION

We discuss our results in three different steps. First, we study the cluster size and the local environment effects on the magnetic moments of pure Fe and Ni clusters. This is followed by our results on  $Ni_nP$  and  $Fe_nC_m$  clusters.

#### A. Pure clusters

In Figs. 3(a) and 3(b) the local densities of states on the central atom site in  $Ni_{13}$  and  $Ni_{43}$  clusters are presented. These results are compared with the density of states (DOS) obtained from band-structure studies<sup>6</sup> in Fig. 3(c).

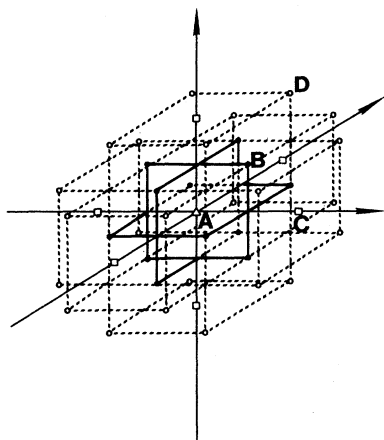


FIG. 1. Geometries of clusters used to model Ni and NiP. The four shells of atoms in the  $\text{Ni}_{43}$  cluster are labeled *A*, *B*, *C*, and *D*.  $\text{Ni}_{13}$  and  $\text{Ni}_{19}$  clusters (not shown) only have shells *A* and *B* and *A*, *B*, and *C*, respectively.  $\text{Ni}_{n-1}\text{P}$  clusters correspond to  $\text{Ni}_n$  clusters with central Ni replaced by P.

The evolution of the DOS with cluster size and the appearance of fine structure in larger clusters are quite apparent. Although the DOS of the  $\text{Ni}_{13}$  cluster contains the salient features found in the band-structure studies, the results of  $\text{Ni}_{43}$  agree much more closely with the bulk value. In the  $\text{Ni}_{13}$  cluster the central atom is surrounded by only one shell of atoms whereas in the  $\text{Ni}_{43}$  cluster, there are four shells of atoms that decorate the central site. We had earlier calculated the DOS in the  $\text{Ni}_{19}$  cluster, which is not too different from that in  $\text{Ni}_{13}$ . This

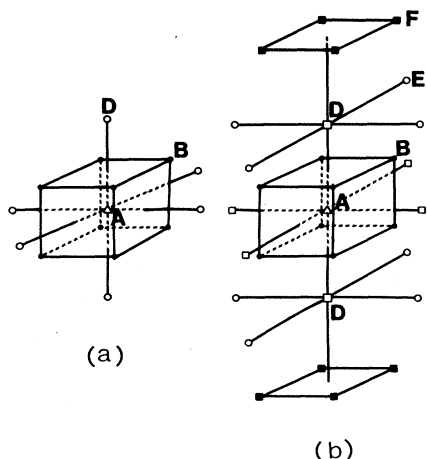


FIG. 2. (a)  $\text{Fe}_{15}$  cluster with *A*, *B*, and *D* shells. The  $\text{Fe}_{14}\text{C}$  cluster has central Fe substituted by *C*. (b)  $\text{Fe}_{31}$  atom cluster used in  $\text{Fe}_{30}\text{C}_2$  model studies. The central Fe is vacant and the two *C* move along the  $[100]$  direction. The  $\text{Fe}_{27}$  cluster (not shown here) is obtained from the  $\text{Fe}_{31}$  cluster by including shells *A*, *B*, *D*, and *E* shown here and adding four atoms to complete the *E* shell around the central site.  $\text{Fe}_{26}\text{C}_2$  is obtained from  $\text{Fe}_{27}$  by substituting a pair of off-centered *C* atoms in place of the central Fe atom.

clearly suggests that for the DOS of the cluster to converge to bulk value, one needs to decorate the central site with at least three nearest shells of atoms. The decoration of the central site can also be looked at from a different perspective. In a fcc lattice, if one includes all the atoms that are nearest to the second shell of atoms in

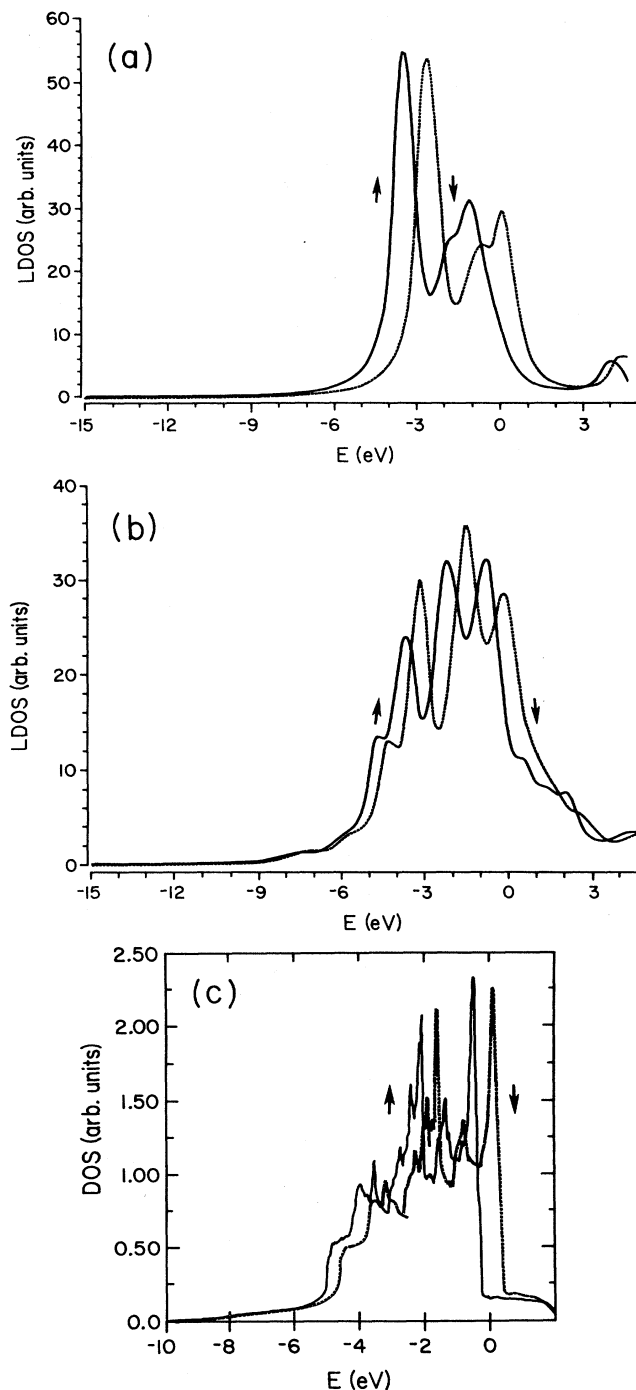


FIG. 3. (a) The local spin density of states on the central site of a  $\text{Ni}_{13}$  cluster. (b) The local spin density of states on the central site of a  $\text{Ni}_{43}$  cluster. (c) The spin density of states of bulk Ni obtained from band-structure calculations of Ref. 6.

Fig. 1, the total number would be 55. In the  $\text{Ni}_{43}$  cluster we are missing one nearest neighbor for every atom in the second shell whereas in the  $\text{Ni}_{13}$  cluster we are missing on the average three nearest atoms. Thus one could also say that for the bulk properties to be realized, both the central site and its nearest neighbors should have their nearest shells complete. This result is consistent with the findings of slab calculations<sup>1,7</sup> where the central layer of a five-layer film has bulklike properties. In Table I we compare the magnetic moments for the central atom (*A*) and those in surrounding shells (*B*, *C*, and *D*) for  $\text{Ni}_{13}$ ,  $\text{Ni}_{19}$ , and  $\text{Ni}_{43}$  clusters. Note that the central site has the lowest moment in all the clusters and that the moments tend to increase as one approaches the surface atoms. The latter trend is due to the decrease in the coordination number as remarked in I. From the  $\text{Ni}_{13}$  to the  $\text{Ni}_{19}$  cluster the central site moment is not changed significantly since only six out of 24 third-nearest-neighbor atoms are present in the  $\text{Ni}_{19}$  cluster. We should remark that our results for  $\text{Ni}_{19}$  as presented here are slightly different from those published earlier.<sup>8</sup> As we had remarked in that paper,<sup>8</sup> the calculated magnetic moments can be reduced by about  $0.3\mu_B$  by placing an attractive potential well that pulls in the electrons. To illustrate this more clearly, we plot in Fig. 4 the moment on the central atom in a  $\text{Ni}_{13}$  cluster as a function of the depth of the attractive potential well. Placing of the potential wells is necessary while modeling a bulk system since the electrons must be confined in such a way that the overlap of the electrons to adjoining cores is minimal. The choice of the depth, however, is not completely unambiguous. We see in Fig. 4 that the moments on the central atom, as well as the average moment per atom in the cluster, converge to a steady value as the well depth increases. In the present calculation we have put a well of depth equal to  $-0.25$  eV since it brings the calculated central moment to closest agreement with experiment. For all subsequent calculations, we have kept the well depth to be constant at  $-0.25$  eV. We also note that the central atom magnetic moment in the  $\text{Ni}_{43}$  cluster is in good agreement with the experimental value of  $0.6\mu_B$ . We recall that the DOS for this site also agreed well with the band-structure value.<sup>6</sup> We could thus conclude that a 43-atom Ni cluster could reproduce bulk features. We find that, analo-

TABLE I. Spin moment and the *d* occupation of various sites (*A*, *B*, *C*, *D*) in the  $\text{Ni}_n$  and  $\text{Ni}_n\text{P}$  clusters (see Fig. 1).

Cluster		<i>A</i>	<i>B</i>	<i>C</i>	<i>D</i>
$\text{Ni}_{13}$	Spin	0.89	1.37		
	<i>d</i> charge	8.69	8.64		
$\text{Ni}_{19}$	Spin	0.86	1.02	1.17	
	<i>d</i> charge	8.76	8.68	8.65	
$\text{Ni}_{43}$	Spin	0.60	0.82	0.91	1.06
	<i>d</i> charge	8.77	8.74	8.69	8.70
$\text{Ni}_{18}\text{P}$	Spin		0.94	1.31	
	<i>d</i> charge		8.70	8.65	
$\text{Ni}_{42}\text{P}$	Spin		0.61	0.82	1.07
	<i>d</i> charge		8.81	8.75	8.69

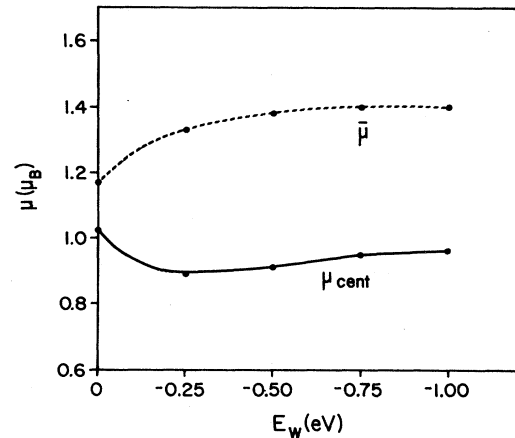


FIG. 4. The spin moment on the central site and the average spin moment of a  $\text{Ni}_{13}$  cluster as a function of depth of the attractive potential well used to simulate bulk effects.

gous to the band-structure results, most of the contributions to the magnetic moments are coming from the *d* electrons. The total charges on the *d* shell calculated from a Mulliken analysis are, however, nearly the same for all atoms in all of the clusters studied.

In Figs. 5(a), 5(b), and 5(c) we plot the DOS for the Ni atoms lying on the second, third, and fourth shells of the  $\text{Ni}_{43}$  cluster, respectively. It is clear that the structure in the DOS begins to disappear as one moves outward. This is caused by a decrease in the coordination number. The DOS for the second shell resembles the central site more closely than any other DOS.

In Figs. 6(a) and 6(b) we present the DOS's at the central site of the  $\text{Fe}_{15}$  and the  $\text{Fe}_{27}$  clusters and compare them to the band-structure results<sup>6</sup> in Fig. 6(c). As in the case of Ni, the central site DOS in the  $\text{Fe}_{27}$  cluster resembles the bulk value more closely than that in the smaller cluster. Even in the  $\text{Fe}_{27}$  cluster, we have a single peak in the DOS at 3 eV for the majority spin which should have split into two peaks to resemble the bulk structure. Thus we conclude that one needs to consider bigger Fe clusters to reproduce the fine structures in the bulk DOS.

In Table II the magnetic moments of the various shells of Fe in  $\text{Fe}_{15}$  and  $\text{Fe}_{27}$  are given. The general trend in the spin and *d*-charge distribution is again the same as observed in Ni, namely, the magnetic moments of atoms on the outer shell are larger than those in the inner shell—a consequence of decreasing coordination number. The magnetic moment of the central atom in the  $\text{Fe}_{27}$  cluster is  $2.47\mu_B$  and does not agree as closely with the experimental value of  $2.2\mu_B$  as observed earlier in Ni. Thus another shell of atoms decorating the central Fe atom is necessary to achieve quantitative agreement with experiment. We note that the DOS in the  $\text{Fe}_{27}$  cluster was also not in perfect agreement with the bulk result.

### B. P impurity in Ni

We next examine the effect of impurities on the host magnetic moment. We first discuss the magnetism of the

NiP system, which is the most widely studied problem in metal-metalloid glasses. We had discussed in a recent paper<sup>8</sup> the mechanism by which the Ni atoms get demagnetized with increasing P concentration. We showed that this arises due to a change in the majority and minority spin population induced by P. Our results were based

upon cluster calculations consisting of up to 19 Ni atoms. Here we present additional results for the Ni<sub>42</sub>P cluster and provide a simple physical picture for the electronic structure.

In Fig. 7(a) we plot the DOS at the P site in the Ni<sub>42</sub>P cluster. It carries a small moment of 0.17 $\mu_B$ , most of which is confined to the P 3s and 3p shells. The P atom has the strongest effect on the magnetic moment of the nearest Ni atoms which decreases from 0.82 $\mu_B$  to 0.61 $\mu_B$  (see Table I). This change is manifested in the spin density of states of the nearest Ni atoms as shown in Fig. 7(b). The effect of P diminishes as one goes outward and the

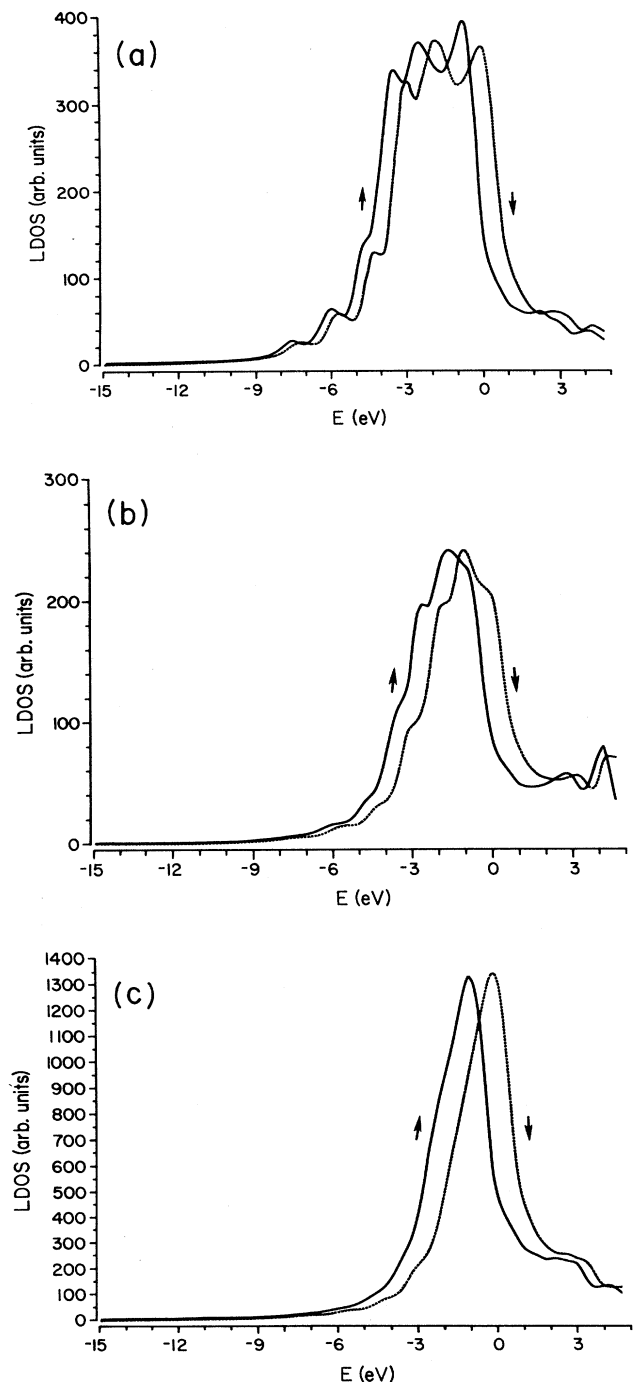


FIG. 5. (a) The local spin density of states on the second shell (B) of a Ni<sub>43</sub> cluster. (b) The local spin density of states on the third shell (C) of a Ni<sub>43</sub> cluster. (c) The local spin density of states on the outermost shell (D) of a Ni<sub>43</sub> cluster.

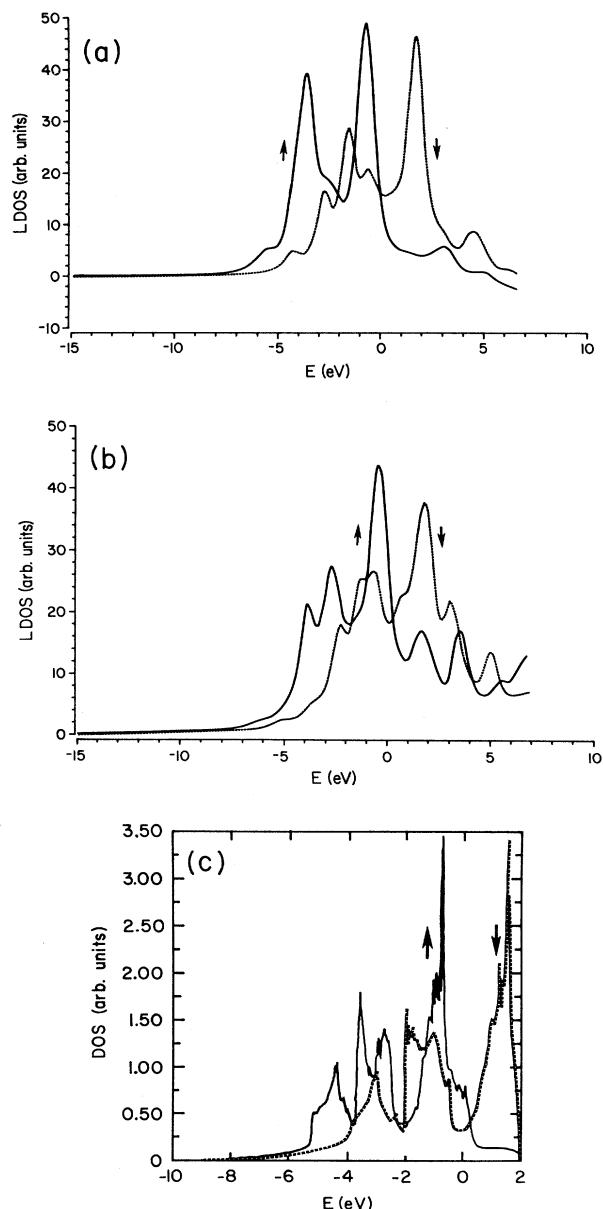


FIG. 6. (a) The local spin density of states on the central site of an Fe<sub>15</sub> cluster. (b) The local spin density of states on the central site of an Fe<sub>27</sub> cluster. (c) The spin density of states of bulk Fe obtained from band-structure calculations of Ref. 6.

TABLE II. Spin moment and the  $d$  occupation of various sites ( $A, B, D, E, F$ ) in  $Fe_n$  and  $Fe_nC_m$  clusters (see Fig. 2).

Cluster		$A$	$B$	$D$	$E$	$F$
$Fe_{15}$	Spin	2.77	3.23	3.48		
	$d$ charge	6.73	6.56	6.55		
$Fe_{27}$	Spin	2.47	2.41	2.90	3.96	
	$d$ charge	6.69	6.67	6.61	6.40	
$Fe_{14}(\text{vacancy})$	Spin		3.33	3.50		
	$d$ charge		6.49	6.53		
$Fe_{14}C_2$	Spin		3.10	3.31		
	$d$ charge		6.54	6.55		
$Fe_{26}C$	Spin		2.46	2.96	3.94	
	$d$ charge		6.65	6.59	6.36	
$Fe_{14}C$ [100]	Spin		2.91	2.70		
	$d$ charge		6.58	6.58		
$Fe_{14}C_2[100]$	Spin		3.11	2.80		
	$d$ charge		6.53	6.56		
$Fe_{26}C_2[100]$	Spin		2.12	2.37	3.98	
	$d$ charge		6.72	6.69	6.40	
$Fe_{30}C_2$ [100]	Spin		2.50	1.75	3.53	3.68
	$d$ charge		6.63	6.89	6.53	6.49

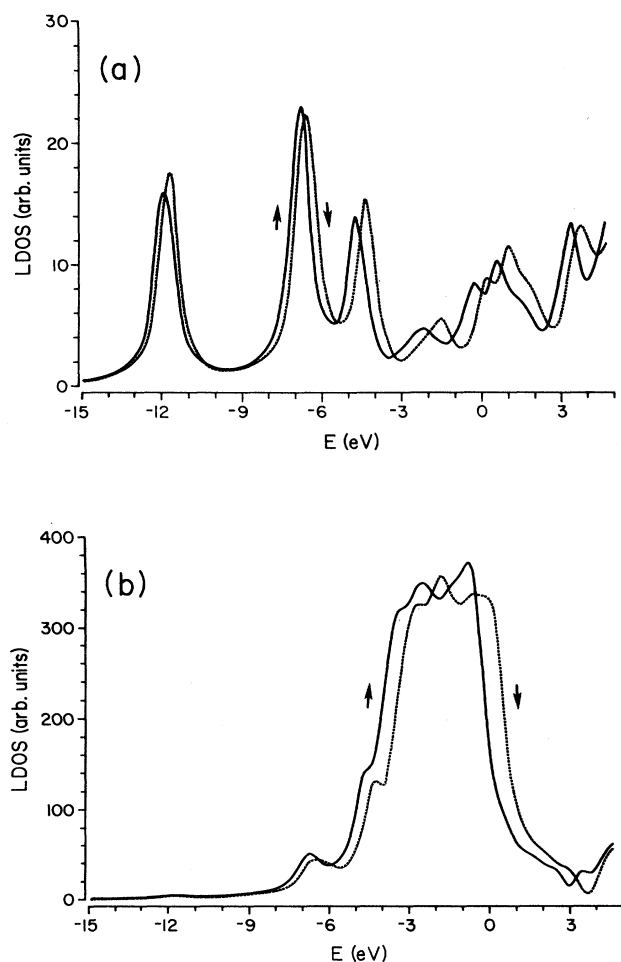


FIG. 7. (a) The local spin density of states on the P site in a  $Ni_{42}P$  cluster. (b) The local spin density of states on Ni sites nearest to P in a  $Ni_{42}P$  cluster.

third layer ( $D$ -shell) atoms in  $Ni_{42}P$  exhibit nearly the same magnetic moment as in the  $Ni_{43}$  parent cluster. This demonstrates that the itinerant Ni electrons screen the P charge within about a lattice spacing.

To understand the origin of the reduction in the host magnetic moment, we give in Table I the magnetic moments of nearest-neighbor Ni atoms due to P in  $Ni_{18}P$  and  $Ni_{42}P$  clusters. The results are compared with the corresponding host  $Ni_{19}$  and  $Ni_{43}$  parent clusters. Note that the net charge on the nearest Ni atom with or without P is not sensitive to cluster size. The situation for the spin occupation is however different. The magnetic moment on the nearest Ni atom (shell  $B$ ) due to P is reduced only by  $0.08\mu_B$  in the  $Ni_{18}P$  cluster from the corresponding value in  $Ni_{19}$ . The reduction, however, is much larger in the  $Ni_{42}P$  cluster where the nearest Ni moment is  $0.4\mu_B$  smaller than the value in the perfect system. This strong cluster size dependence of  $\mu_B$  arises due to the interaction of Ni atoms with the embedding potential incorporated to simulate the crystalline environment. In the  $Ni_{18}P$  cluster the  $B$ -shell atoms are separated from the embedding atoms by only one shell of atoms, whereas in the  $Ni_{42}P$  cluster there are two shells of atoms separating the  $B$ -type atoms from the embedding medium. Thus the magnetic moment of  $B$ -shell atoms in the  $Ni_{42}P$  cluster is influenced much less by the embedding potential than that in the  $Ni_{18}P$  cluster. Since the embedding atoms are magnetic, their interaction with cluster surface atoms makes them more magnetic. A second point to note is that while the net charge on the Ni atom does not change significantly with or without P, the magnetic moment undergoes appreciable modification. Since most of the charge and the spin reside on the  $3d$  shell, it is clear that the reduction in the moment is caused by transfer of electrons from majority to minority spin band and not due to any charge transfer between P and Ni. This result is particularly evident from the  $Ni_{43}$

cluster. As we have indicated earlier,  $\text{Ni}_{43}$  is a large enough cluster to simulate the bulk electronic properties.

### C. Point defects in Fe

We have considered three kinds of defects; a monovacancy, carbon-monovacancy complex with carbon occupying various positions with respect to the vacancy center, and polycarbon vacancy complexes. In Table II we note that the moment on the nearest-neighbor Fe atom (*B* shell) in  $\text{Fe}_{14}$  due to the vacancy increases while the moment at the next-near-neighbor shell (*D* shell) remains practically unchanged. As pointed out in I, the enhancement of the moment in the *B* shell is caused by a reduction in overlap between atomic orbitals. The second shell (*D*) is shielded from the vacancy by the eight Fe atoms in the *B* shell and consequently is unaffected. The introduction of carbon at the center of the vacancy, however, has the opposite effect,<sup>9</sup> causing the nearest-neighbor moment to decrease. This is caused by the interaction of the carbon *3p* with the Fe *3d* orbitals. As discussed for P in Ni, the decrease in the moment is due to the transfer of spins from majority to minority states and not due to any charge transfer between carbon and Fe atoms.

There is theoretical<sup>10,11</sup> as well as experimental evidence<sup>12</sup> that the equilibrium position of carbon is at an off-center vacancy site. To illustrate how this affects the magnetic moment, we plot in Fig. 8 the magnetic moments of the Fe atoms in the *B* and *D* shells of an  $\text{Fe}_{14}\text{C}$  cluster with carbon moving along the [100] direction from the vacancy center. At the origin (carbon at the vacancy center), the moment of the *D* shell is slightly higher than the *B* shell as seen in Table II. As carbon moves, the moments on both the shells tend to decrease and assume a single value for a displacement of around 1.6 a.u. At this position, carbon is equidistant from the Fe atoms on the *D* shell and the four Fe atoms on the *B* shell that share the corners closest to carbon. Beyond this position, the carbon distance from the body center Fe decreases

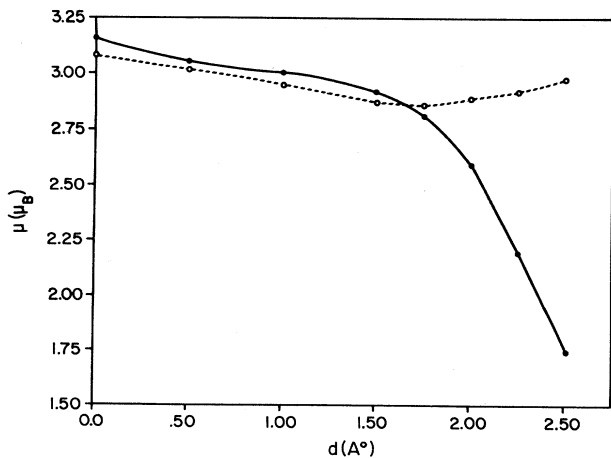


FIG. 8. The magnetic moment of the Fe atoms in the *B* and *D* shells of the  $\text{Fe}_{14}\text{C}$  cluster as a function of the C position along [100] direction.

much faster than its distance from the other four atoms discussed above. Consequently, there is a sharp decrease in the magnetic moment of the nearest Fe atom—a consequence of strong overlap between carbon *3p* and Fe *3d* orbitals.

To further illustrate that the charge transfer between C and Fe does not play a role in the strong dependence of Fe moment on Fe-C distance, we note that in Table II the *3d* charge on all Fe atoms with or without carbon is  $6.6 \pm 0.1$ .

We have also calculated the energetics of carbon moving along various symmetry directions. Contrary to earlier assumptions, we found that<sup>11</sup> the equilibrium configuration of carbon is along a special direction given by  $[y = x \pm a/4]$  where *a* is the lattice spacing. In this direction, carbon is at a distance of 3.35 a.u. from the vacancy center and has three nearest-neighbor Fe atoms. The moment on these atoms is reduced to  $2.5\mu_B$  whereas for the equilibrium position along [100] the corresponding moment is  $2.9\mu_B$ . Experiments on positron annihilation<sup>12</sup> have been carried out to locate the equilibrium site of carbon. While the experiment clearly suggests that carbon is situated at an off-center vacancy site, it cannot distinguish between the equilibrium sites along [100] or  $[y = x \pm a/4]$ . This is because the positron lifetimes for carbon at the minimum in these directions are nearly the same. It will, therefore, be useful to probe, experimentally, the magnetic moment in carbon vacancy complexes in Fe since we demonstrate that the moments are clearly different for these two sites. No experimental data are available at this time.

Positron annihilation studies<sup>12</sup> as well as theoretical calculations<sup>11</sup> have also suggested that a vacancy in Fe is capable of trapping more than one C atom. We have therefore studied the effect of carbon decoration on the magnetic moment in  $\text{Fe}_{14}\text{C}_2$  and  $\text{Fe}_{26}\text{C}_2$  clusters. The results are again presented in Table II. We first point out that the atoms on the *D* and *E* shells in pure Fe clusters are each split into two subsets in clusters containing two carbon atoms. This is caused by the fact that as each C atom occupies an off-center position, four of the six atoms in the *D* shell are at a different distance from the carbon atom than the other two. In Table II we only give the moment on those Fe atoms that are closest to carbon.

We begin by comparing the results for  $\text{Fe}_{14}\text{C}$  [100] and  $\text{Fe}_{14}\text{C}_2$  [100] clusters. In both of these clusters, the carbon atom(s) occupies the minimum energy configuration along the [100] direction from the vacancy center. Note that the magnetic moment as well as the charge of the *3d* shell on the Fe atoms on both the *B* and *D* shells are nearly the same. This illustrates that the decoration of vacancy by more than one carbon has little effect on the electronic structure of Fe atoms. The interaction of carbon with its nearest-neighbor Fe atoms is much larger than between the two carbon atoms. A second point to note is that while the moment on the *B* shell is reduced by only  $0.2\mu_B$  due to carbon, the moment on the *D* shell is reduced by as much as  $0.6\mu_B$ . This is due to the fact that carbon along the [100] direction is closer to the Fe atom on the *D* shell than to the Fe atoms on the *B* shell. The same trend is preserved in the larger cluster  $\text{Fe}_{26}\text{C}_2$

although the difference in the moments between the  $B$  and  $D$  shell atoms are somewhat different. This is caused by the effect of an additional 12 surface atoms in the  $\text{Fe}_{26}\text{C}_2$  cluster. The magnetic moment on the outermost shell of the  $\text{Fe}_{26}\text{C}_2$  cluster is nearly identical with the  $\text{Fe}_{27}$  cluster. Thus the effect of carbon on the electronic structure of Fe is short ranged due to an efficient screening of the charge by the host conduction electrons. In all the clusters in Table II, small or large, perfect or defected, the charges on the  $3d$  electrons are nearly the same whereas the magnetic moments change over a wide margin. This result, which is analogous to the NiP system discussed earlier,<sup>8</sup> clearly demonstrates that the dominant interaction of the impurity with host magnetic moment is primarily of magnetic origin. The charge transfer between impurity and host atoms does not play a major role—contrary to what is known in metal-hydrogen systems. In the following, we describe a simple physical model to account for the observed magnetic properties. We note that in both  $\text{Fe}_{14}\text{C}_2$  and  $\text{Fe}_{26}\text{C}_2$  clusters, the Fe atom directly above carbon in the  $D$  shell does not have all of its nearest-neighbor Fe atoms. To calculate a more accurate value of the magnetic moment of this Fe atom, we have used an  $\text{Fe}_{30}\text{C}_2$  cluster by decorating the above atom with an additional four atoms (see Fig. 2). The results in Table II indicate that the moment of the atom on the  $D$  shell is further reduced to  $1.75\mu_B$ . Thus, for an accurate determination of the magnetic moment of a host atom due to an impurity, it is necessary to choose a cluster which has at least the first near neighbors of the magnetic atom, under study, complete.

#### D. Simple theoretical model

To provide a qualitative picture for the mechanism of spin quenching we give a schematic plot of the host density of states as well as the impurity atomic levels in Fig. 9(a). The interaction as remarked earlier is between impurity  $p$  levels and the host  $d$  band. The lower-lying impurity  $s$  states are somewhat broadened but do not overlap with the host conduction states. The major electronic change occurs due to  $p$ - $d$  hybrids formed out of the bonding and antibonding interaction of impurity  $p$  and host  $d$  electrons as shown in Fig. 9(b). There are two sets of  $p$ - $d$  hybrids belonging to majority and minority spin states. Since the majority band is full, the  $pd$  hybrid corresponding to the majority spin cannot accommodate all of the electrons in the bonding state and some of these have to occupy an antibonding state. If these antibonding states are above the Fermi energy, the majority electrons occupying these states would fall to lower states reserved for minority spins. This transfer would then set up a mechanism for converting majority spins into minority spins resulting in a reduction in the magnetic moment while maintaining the total charge. This behavior of density of states has been witnessed in our computed density of states discussed earlier.

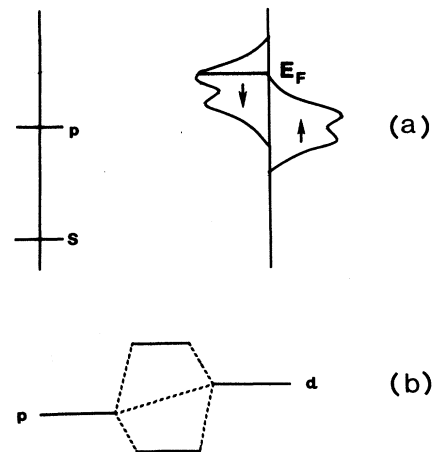


FIG. 9. Schematic diagram showing the interaction between impurity (C or P)  $s$  and  $p$  levels and the  $d$  band of the host (Fe or Ni). (a) shows the impurity levels and the host band while (b) shows the  $pd$  hybrids.

#### IV. CONCLUSIONS

We have carried out self-consistent cluster calculations of the magnetic properties of Fe and Ni containing impurities. Following is a summary of our results.

- (1) The magnetic moment of the central atom in the cluster can nearly equal its bulk value if it is surrounded by three or more nearest-neighbor shells.
- (2) The magnetic moment increases as the number of host atoms surrounding the site under investigation decreases.
- (3) Nonmagnetic impurities such as phosphorous and carbon have a significant effect on the magnetic moment of the nearest host atom causing a sharp reduction from its value in the perfect state.
- (4) The quenching of the moment is caused by a transfer of majority spin electrons in the host impurity hybrid band to the minority states. This quenching could be accomplished without requiring a transfer of charge from impurity to the host and thereby prohibiting a rise in the Fermi energy. Current experiments<sup>13</sup> tend to support this picture.
- (5) The effect of the impurity on the host magnetic properties is of short range and confined to the nearest atoms.
- (6) Formation of defect complexes appears to play a less significant role in the distribution of the host magnetic moment.

#### ACKNOWLEDGMENTS

This work was supported by the Army Research Office under Grant No. DAAL 03-89-K-0015.

- <sup>1</sup>F. Liu, M. R. Press, S. N. Khanna, and P. Jena, Phys. Rev. B **39**, 6914 (1989).
- <sup>2</sup>D. M. Cox, D. J. Trevor, R. L. Whetten, E. A. Rohlfing, and A. Kaldor, Phys. Rev. B **32**, 7290 (1985).
- <sup>3</sup>E. Kneller, *Ferromagnetismus* (Springer, Berlin, 1962), p. 148; J. J. Becker, F. E. Luborsky, and J. L. Walter, IEEE Trans. Magn. **Mag-13**, 988 (1977); W. A. Hines, K. Glover, W. G. Clark, L. P. Kobacoff, C. U. Modezelewski, R. Hasegawa, and P. Duwez, Phys. Rev. B **21**, 3771 (1980); P. W. Selwood, *Chemisorption and Magnetization* (Academic, New York, 1974).
- <sup>4</sup>D. E. Ellis, Int. J. Quantum Chem. S **2**, 35 (1968); D. E. Ellis and G. S. Painter, Phys. Rev. B **2**, 2887 (1970); D. E. Ellis, G. A. Benesh, and E. Byrom, *ibid.* **16**, 3308 (1977).
- <sup>5</sup>G. A. Benesh and D. E. Ellis, Phys. Rev. B **24**, 1603 (1981); M. R. Press, Ph.D. thesis, Northwestern University, 1986.
- <sup>6</sup>V. L. Moruzzi, J. F. Janak, and A. R. Williams, *Calculated Electronic Properties of Metals* (Pergamon, New York, 1978).
- <sup>7</sup>A. J. Freeman, J. Magn. Magn. Mater. **35**, 31 (1983).
- <sup>8</sup>M. R. Press, S. N. Khanna, and P. Jena, Phys. Rev. B **36**, 5446 (1987).
- <sup>9</sup>P. Blaha and J. Callaway, Phys. Rev. B **33**, 1706 (1986).
- <sup>10</sup>K. Masuda, Phys. Status Solidi B **116**, 9 (1983); M. J. Puska and R. M. Nieminen, J. Phys. F **12**, L211 (1982); R. A. Johnson and A. C. Damask, Acta Metall. **12**, 443 (1964).
- <sup>11</sup>M. R. Press, S. N. Khanna, and P. Jena (unpublished).
- <sup>12</sup>A. Vehanen, P. Hautojarvi, J. Johansson, J. Yli-Kaupilla, and P. Moser, Phys. Rev. B **25**, 762 (1982).
- <sup>13</sup>J. Bakonyi, H. E. Schone, L. K. Varga, K. Tompa, and A. Lovas, Phys. Rev. B **33**, 5030 (1986); E. Belin, A. Traverse, A. Szasz, and F. Machizaud, J. Phys. F **17**, 1913 (1987); I. Bakonyi, H. Ebert, W. Socher, J. Voitlander, E. Wachtel, N. Willmann, and B. Predel, J. Magn. Magn. Mater. **68**, 47 (1987).